Proceeding of the IEEE
International Conference on Robotics and Biomimetics
Dali, China, December 2019

RGB-Thermal Fusion Network for Leakage Detection of Crude Oil Transmission Pipes

Anqi Li[1], Dongxu Ye[1], Erli Lyu[1], Shuang Song[1],
Max Q.-H. Meng[2], *Fellow, IEEE*, Clarence W. de Silva[3]*, *Fellow, IEEE*

***Abstract*—Detection and diagnosis of defects in pipelines that transmit crude oil is crucial for assuring the safety and integrity of crude oil transportation. With the development of deep learning technologies, studies have been done in the application of neural networks to the defect detection of crude oil transmission pipeline. However, most of the image-based detection research use RGB images from optical cameras to make decisions, and their outcomes are easily influenced by poor lighting conditions. Further more, RGB images provide only an external view of the pipe while the pipeline defects can be within the structure. In order to obtain a high accuracy and robust classification for the leakage level in crude oil transmission pipelines, the present paper takes advantages of thermal images and fuses them with RGB images using a novel convolutional network (CNN). Specifically, the paper proposes an intelligent network architecture-based CNN to which the features of RGB images and thermal images are integrated. The experimental results verify that the proposed method provides outstanding performance in the leakage level classification for crude oil pipe.**

***Index Terms*—crude oil pipelines; leakage level detection; convolutional neural networks; thermal images; RGB images; feature map fusion.**

I. Introduction

In recent years, with the rapid growth of crude oil production and consumption, the speed of pipeline transportation development has been accelerating. The safety of pipeline transportation has gradually become a global focused issue [1]. As a pipeline gets older, it is affected by inevitable corrosion, wear and other natural or man-made damage, and as a result, pipeline structural integrity suffers leading to leakage [2], this will not only cause huge economic losses and environmental pollution, but also threaten human safety [3]–[5]. Therefore, leakage detection of crude oil transmission pipes has a very important practical significance.

At present, commonly manual methods are used in the assessment of oil leaks in pipelines. Human inspectors walk alongside the pipes to visually check them and record any problems such as corrosion, fracture and leaks [6], [7]. Traditional fault diagnosis methods are rely heavily on the diagnosis experience of workers. In order to achieve automatic detection of leakage in crude oil pipelines, some technological advancements have been made. Lowe et al. [8] summarized wave propagation methodology and its sensitivity to pipeline defects, which provided a scientific basis for defect detection method using guided waves. Singh et al. [9] developed a risk inspection program based on a fuzzy logic framework to help maintenance engineers take necessary preventive measures before the actual accidents occur. Simpson et al. [10] designed a radio frequency identification system to complete the detection task of a humidity sensor for detecting oil leakage.

During the past few years, machine learning technology has developed rapidly, and the focus of pipeline detection has gradually shifted from signal processing to various machine learning techniques. Zhang et al. [11] proposed a defect detection approach based on the improved Faster R-CNN network and they also used K-means algorithm to improve the accuracy of the pipeline detection method further. Ouadah et al. [12] applied machine learning and a multi-criteria decision making approach to carry out defect risk ranking of a pipeline. Mohamed et al. [13] proposed an approach based on decision tree for defect detection and classification in oil pipelines, and they used complexity MLF data. A major drawback in most current methods of defect detection of crude oil pipeline is that it is difficult to obtain and process the original information, and the use of sensors and other methods still need superabundant feature extraction from raw data. Among most of the machine learning methods, CNN, as an important approach of deep learning, has been used widely in various fields. It performs well in image classification notably because of its ability to automatically extract features [14]. In addition, recent research has shown that image fusion can provide more detailed information thereby improving the performance of CNN [15].

The paper fully exploits the advantages of thermal images, and fuses thermal images with RGB images using a CNN model to achieve an accurate and robust leakage level classification model for crude oil transmission pipes. The main innovation of this paper is the CNN structure for fusing two types of images. The CNN model extracts representative features automatically from raw images, and the images are fused in the feature map stage in this model to increase the reliability of classification. The performance of the proposed

[1]Anqi Li, Dongxu Ye, Erli Lyu, and Shuang Song are with School of Mechanical Engineering and Automation, Harbin Institute of Technology(Shenzhen), Shenzhen, China, 518055.

[2]Max Q.-H. Meng is with Department of Electronic Engineering, the Chinese University of HongKong, HongKong, China, and affiliated with the State Key Laboratory of Robotics and Systems (HIT), Harbin Institute of Technology, China.

[3]Clarence W. de Silva is with Department of Mechanical Engineering, the University of British Columbia, Vancouver, Canada.

*Corresponding author: Clarence W. de Silva, mail: desilva@mech.ubc.ca

978-1-7281-6321-5/19//$31.00 ©2019 IEEE

CNN framework is evaluated through simulated experiment of pipeline leakage and a comparative model. The remainder of this paper is structured as follows. In section II, data acquisition is presented. In section III, the details of the proposed network are reviewed. Section IV describes and discusses the experimental results. The conclusions of the work are presented in the last section.

II. Data acquisition

A. Experiment Platform

The joints of crude oil transmission pipes are prone to leakage mainly because of the phenomenon of stress concentration [7]. In order to obtain adequate images data for training, an experiment platform is designed with a fire hydrant with flange joint and a combined pipe with two types of common pipe joints: welded joint and threaded joint. The experiment setup is shown in Fig. 1. This study uses X2 optical camera (Shenzhen electronic technology) and NC160 thermal camera (Shanghai Noble) to acquire RGB images and thermal images, respectively. RGB images obtained from the optical camera with wider shooting angle is cropped to align two kinds of images approximately. In the process of the data acquisition, different temperatures and volumes of oil flow are imparted at different joints. RGB images and thermal images are taken simultaneously from different angles at multiple joints of the transmission pipes.

Fig. 1. Experiment platform.

Because of the physical similarity between engine oil and crude oil, engine oil used instead of crude oil in the experiments. Since the crude oil is heated with steam during transportation, the oil used in the experiments is heated to 70°C before application. A water bath heating device is used to heat oil to the specified temperature. In the present study, the leakage condition is divided into four levels, including three leak conditions (minor leak, moderate leak, large leak) and a normal condition (no leak). Given that at a pipe crack the leakage is small, and is relatively less than in other leak conditions. The leaking oil will flow slowly down the outer wall of the pipe and cool down quickly to a certain temperature that is determined by both environmental temperature and the oil temperature. In addition, the temperature of the outer pipe wall is controlled at around 35°C in the experiments. The parameters of the experiment are shown in Table I.

TABLE I
THE PARAMETERS OF THE EXPERIMENT

Leakage Level	Temperature of oil (°C)	Volume of oil (ml)	RGB images	Thermal images
Large leak	70	10–15	172	172
Moderate leak	70	6–8	220	220
Minor leak	25	2–3	253	253
No leak		0	365	365

B. Data Preprocessing

Many factors can affect the performance of CNN, among which one of the most important factors is whether the original data is sufficient and representative. At the beginning of data preprocessing, the flip technique is used to augment the dataset from 1010 RGB images and 1010 thermal images to form 2020 images. 344×2 are large leaks, 440×2 are moderate leaks, 506×2 are minor leaks, and 730×2 are no leaks (×2 represents RGB images and thermal images). In order to ensure the uniform size of feature map when they are fused in the CNN model, RGB images and thermal images are cropped to a uniform size of 200×200. The RGB and thermal images taken at the same time should be spliced together (RGB is on the left, and thermal image is on the right) to form one picture of size 200×400 in the preprocessing stage to ensure that the two types of images input into the network are of one-to-one correspondence. In this study, 60% of the samples are used for training, 20% for validation, and 20% for testing. The training dataset can be used to train the CNN model by minimizing the error between the true value and the predicted value. The validation dataset selects the appropriate model by adjusting hyper parameters. The testing dataset is used for evaluating the generalization ability of the selected CNN model. The details of each level are given in Table II.

TABLE II
THE DETAILS OF DATASET

Leakage Level	Class label	Training samples	Validation samples	Testing samples	Total
Large leak	0	208	68	68	344
Minor leak	1	304	102	100	506
Moderate leak	2	264	88	88	440
No leak	3	438	146	146	730
Total		1214	404	402	2020

III. Proposed network

This paper proposes a novel leakage detection approach for crude oil transmission pipes based on RGB-Thermal fusion CNN framework. The key point of this paper is to make full use of the advantages of RGB image and thermal image to realize information fusion in the CNN model and achieve better classification performance. Fig. 2 shows the overall flowchart of the proposed detection approach.

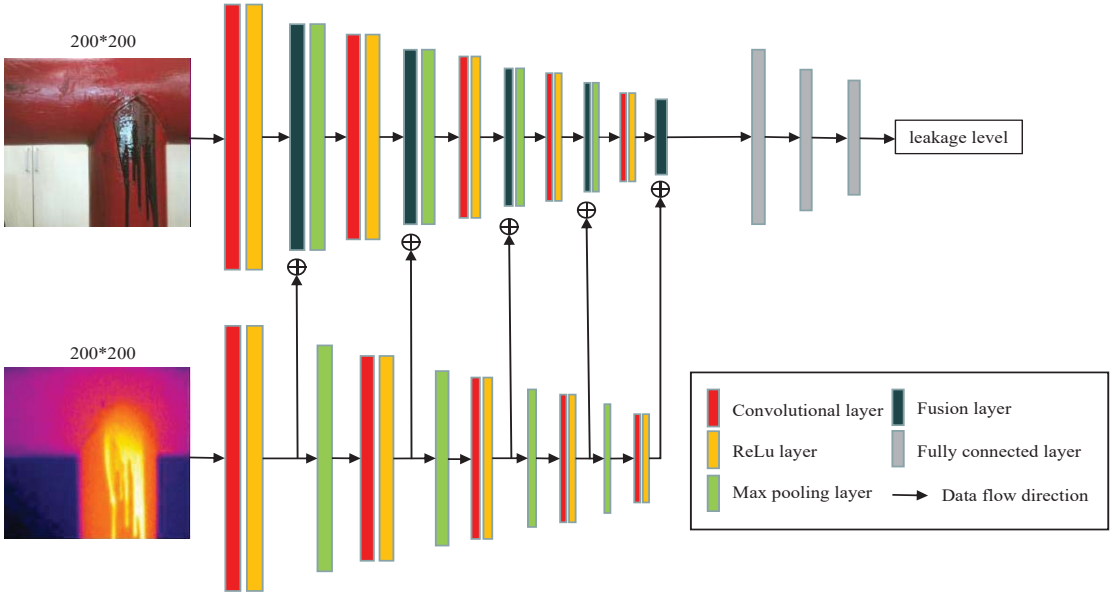

Fig. 3. Architecture of RGB-Thermal fusion network.

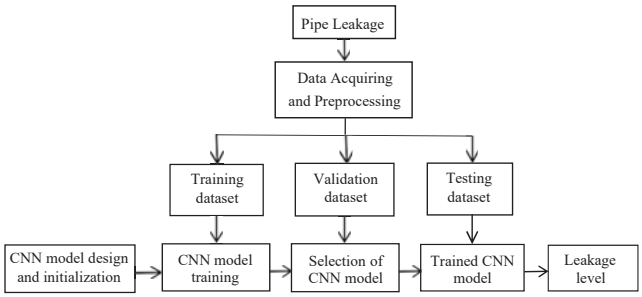

Fig. 2. Flowchart of the proposed detection approach.

The detailed structure of RGB-Thermal fusion CNN is shown in Fig. 3. Unlike traditional methods, which need manual features to classify different conditions, the present method has a strong ability of automatic feature extraction. Convolutional layer with multiple convolutional kernels can extract features from the input image by the convolution operation. In this paper, two feature extraction routes are designed in the network structure, which are used to extract feature information from RGB images and thermal images, respectively. Then a nonlinear activity function is applied to the output from the previous convolutional layer. ReLU function is adopted in this paper because of its excellent performance in the recent studies on classification task [16]. ReLU can be presented by the following equation:

$$F(x) = \max(0, x) \tag{1}$$

RGB-Thermal fusion is achieved after the ReLU layer by stacking the feature map extracted from the RGB images and the thermal images in the RGB route. Followed by the fusion layer is the max pooling layer, which can reduce the dimension of the feature map and the parameters of the network [17]. Max pooling kernel of size 2×2 with step size 2×2 is used in this paper. The max pooling expression is given by Equation (2). Followed by another such stage, the difference between these stages is the parameter design of each layer.

$$y_{ijf} = \max\left(y_{ijf} : i \le i' \le i+h, j \le j' \le j+w\right) \tag{2}$$

where h and w are the height and the width of the max pooling kernel, respectively, and f represents the index of the feature map. The maximum value in the region is selected as the target value.

At the end of the network is the fully connected layer, which integrates the information extracted from the previous layers. It plays the role of classifier in the whole network. The output of the last fusion layer is used as the input of the fully connected layer. Over-fitting problems often occur during the training stage, especially in the case of limited training data, which will lead to high accuracy on the training dataset but poor performance on the testing dataset. In this paper, dropout [18] and L2-regularization methods are adopted to solve over-fitting in the fully connected layer. Because the proposed network is not as deep as VGG, 5×5 filter is adopted in the first two layers to acquire more informations and avoid overfitting at the same time. The hyper parameters of convolution layers are shown in Table III.

The parameters in the network such as weight and bias are updated using the gradient descent method, as given by the following expressions:

$$W^{(j)} = W^{(j-1)} - \eta \frac{\partial}{\partial W} J(W, b) \tag{3}$$

$$b^{(j)} = b^{(j-1)} - \eta \frac{\partial}{\partial b} J(W, b) \tag{4}$$

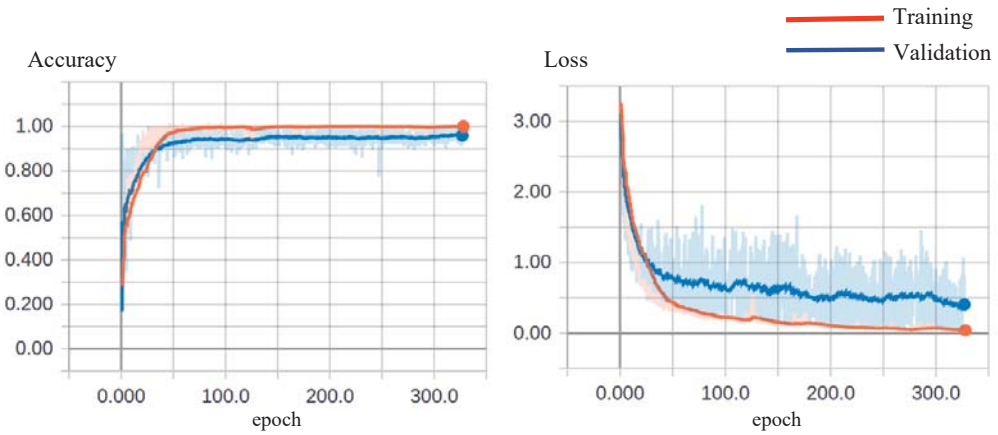

Fig. 4. Accuracy curve(left) and loss curve(right) in the training stage(red) and validation stage(blue).

where η represents the learning rate; W and b represent the weight and bias, respectively; and J is the loss function of the CNN model.

TABLE III
THE HYPER PARAMETERS OF CONVOLUTION LAYERS

	Parameter	conv1	conv2	conv3	conv4	conv5
RGB	Size of filters	5×5	5×5	3×3	3×3	3×3
	Number of filters	64	128	256	512	1024
	Stride	1×1	1×1	1×1	1×1	1×1
Thermal	Size of filters	5×5	5×5	3×3	3×3	3×3
	Number of filters	64	128	256	512	1024
	Stride	1×1	1×1	1×1	1×1	1×1

IV. EXPERIMENT RESULTS AND DISCUSSIONS

The present experiments adopt python as programming language and Tensorflow 1.9.0 with the CUDA 9.0 and cudnn 7.3.1 libraries as the experimental environment. The complex data structure is transferred to the artificial intelligence neural network for analysis and processing. The proposed network runs on a computer with Intel 2.4GHz CPU and a NVIDIA GTX 1080TI graphics card for training.

In the training process, randomly shuffled samples are fed into the network for training. Initialization is implemented using Xavier method [19] for the developed RGB-Thermal fusion network. To avoid over-fitting, the ratio of dropout is set to 0.5 in the first two fully connected layers. The parameters are updated according to the backward propagation algorithm [20] to obtain a suitable CNN model. The Adam optimizer [21] is used to update weights and optimize the network. The initial learning rate is set to 0.0001. With the increase of the training epoch, the piecewise-constant learning rate decay is adopted in this paper, and it is multiplied by 0.99 every 100 epochs. The training is stopped when the loss of the model is minimized and convergence is achieved. In the validation stage, an optimal CNN model is selected according to the performance of the validation set. Fig. 4 depicts the curve of loss and accuracy in training stage and validation stage,respectively. From the Fig. 4 we can see that the model converges at around 200 epochs.

Confusion matrix in the testing dataset is shown in Fig. 5. The testing dataset performed well on the trained RGB-Thermal fusion model, with just a small number of testing samples misclassified. Further comparative analysis of the proposed RGB-Thermal fusion network is provided next.

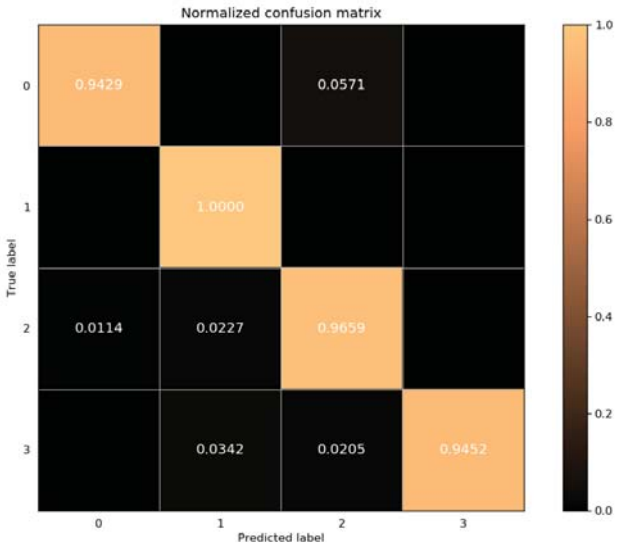

Fig. 5. Leakage classification confusion matrix.

Four kinds of evaluation indicators are adopted to evaluate the performance of the proposed RGB-Thermal fusion model, namely precision (P), recall (R), F1-score (F1) and average accuracy (Acc) of each method. The first three evaluation indicators are calculated by the following formula, and Acc is the average accuracy of each method.

$$P = \frac{TP}{TP+FP} \tag{5}$$

TABLE IV
THE COMPARISON RESULTS USING DIFFERENT NETWORK

Method	Large leak			Moderate leak			Minor leak			No leak			Acc
	Precision	Recall	F1-score	Precision	Recall	F1-score	Precision	Recall	F1-score	Precision	Recall	F1-score	
LeNet-5 (3c)	80.00	76.47	78.20	68.89	70.45	69.66	70.59	84.00	76.71	94.53	82.88	88.32	79.35
LeNet-5 (4c)	91.94	83.82	87.69	84.54	93.18	88.65	81.36	96.00	88.07	98.40	84.25	90.77	89.06
AlexNet (3c)	70.83	75.00	72.86	70.89	63.64	67.07	71.76	94.00	81.39	98.33	80.82	88.72	79.35
AlexNet (4c)	96.55	82.35	88.89	80.77	95.45	87.50	92.93	92.00	92.46	96.45	93.15	94.77	91.54
VGGNet16 (3c)	87.30	80.88	83.97	68.89	70.45	69.66	76.47	78.00	77.23	91.84	92.47	92.15	82.09
ResNet50 (3c)	87.69	83.82	85.71	67.77	93.18	78.47	87.21	75.00	80.65	97.69	86.99	92.03	84.83
RGB-Thermal fusion network	98.51	94.29	96.35	92.39	96.59	94.44	93.46	100.00	96.62	100.00	94.52	97.18	96.23

$$R = \frac{TP}{TP+FN} \tag{6}$$

$$F1 = \frac{2 \times P \times R}{P+R} \tag{7}$$

here TP, FP, FN represents True Positives, False Positives, and False Negatives, respectively.

The RGB-Thermal fusion network is compared with LeNet-5 [22], AlexNet [23], VGGNet16 [24], and ResNet50 [25] in the leakage level classification. These compared models use the same dataset as the RGB-Thermal fusion network. All models are trained until they converge. 3c and 4c, respectively, represent that the CNN model uses 3 channels RGB image samples and 4 channels RGB-Thermal fusion image samples. The detailed comparative results are shown in Table IV. The superiority of the RGB-Thermal fusion network can be seen from the results presented in Table IV. It is observed that the evaluation indicators of the proposed model are all above 90%, and more than half of the evaluation indicators are over 95%. The average accuracy of the proposed network is 96.23%, which is much higher than in the other methods.

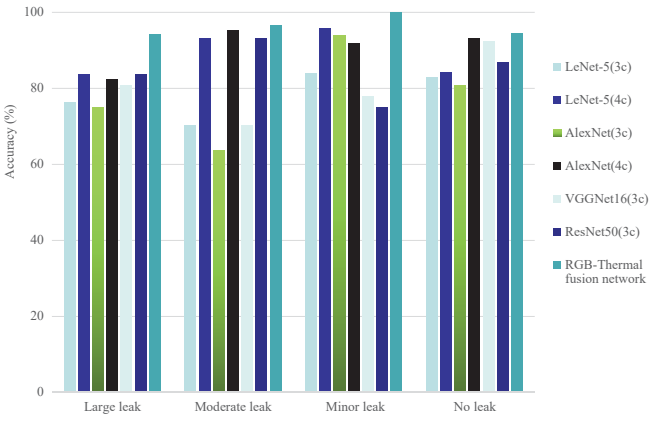

Fig. 6. Accuracy comparison results of different methods.

In order to further verify the feasibility of the RGB-Thermal fusion network, the accuracy of each leakage level is compared using different methods in Fig. 6. It can been seen that the proposed model is superior to the other models in all four leakage types. This result verifies that the present model has better accuracy and robustness, it can accurately classify the leakage level in crude oil transportation pipeline.

V. CONCLUSION

In this paper, a RGB-Thermal fusion network was proposed for the leakage detection of crude oil transmission pipes. The proposed model was able to realize the automatic leakage level classification. The features automatically extracted from RGB images and thermal images were fused in the proposed model. The model integrated the information of RGB images and thermal images, which not only improved the classification ability, but also solved the insufficient single source image information problem. The experimental results verified the superior performance of the proposed network in the application of crude oil transmission pipeline leakage level classification. Compared with other classic network used for classification, it was shown that the proposed model had higher accuracy and robustness in the leakage detection in crude oil transmission pipes.

REFERENCES

[1] L. Boaz, S. Kaijage, and R. Sinde, "An overview of pipeline leak detction and location systems," in *Proceedings of the 2nd Pan African International Conference on Science, Computing and Telecommunications (PACT 2014)*. IEEE, 2014, pp. 133–137.

[2] L. Ma, L. Cheng, and M. Li, "Quantitative risk analysis of urban natural gas pipeline networks using geographical information systems," *Journal of Loss Prevention in the Process Industries*, vol. 26, no. 6, pp. 1183–1192, 2013.

[3] A. Aljaroudi, F. Khan, A. Akinturk, M. Haddara, and P. Thodi, "Risk assessment of offshore crude oil pipeline failure," *Journal of Loss Prevention in the Process Industries*, vol. 37, pp. 101–109, 2015.

[4] K. Lee, M. Boufadel, B. Chen, J. Foght, P. Hodson, S. Swanson, and A. Venosa, "The behaviour and environmental impacts of crude oil released into aqueous environments," *Ottawa: The Royal Society of Canada*, 2015.

[5] J. Liu, J. Yao, M. Gallaher, J. Coburn, and R. Fernandez, "Study on methane emission reduction potential in chinas oil and natural gas industry," Tech. rep., April, Tech. Rep., 2008.

[6] T. Slade, Y. Okamoto, J. Talor *et al.*, "Economic benefits of leak detection systems: A quantitative methodology," in *PSIG Annual Meeting*. Pipeline Simulation Interest Group, 2014.

[7] M. A. Karimi and A. Shamim, "Smart clamp-type microwave sensor for accidental leak detection from pipe joints."

[8] M. J. Lowe, D. N. Alleyne, and P. Cawley, "Defect detection in pipes using guided waves," *Ultrasonics*, vol. 36, no. 1-5, pp. 147–154, 1998.

[9] M. Singh and T. Markeset, "A methodology for risk-based inspection planning of oil and gas pipes based on fuzzy logic framework," *Engineering Failure Analysis*, vol. 16, no. 7, pp. 2098–2113, 2009.

[10] A. S. Hashim, B. Grămescu, and C. Niţu, "Pipe leakage detection using humidity and microphone sensors–a review," in *International Conference of Mechatronics and Cyber-Mixmechatronics*. Springer, 2018, pp. 129–137.

[11] Z.-j. ZHANG, B.-a. LI, X.-q. LV, and K.-h. LIU, "Research on pipeline defect detection based on optimized faster r-cnn algorithm," *DEStech Transactions on Computer Science and Engineering*, no. ammms, 2018.
[12] A. Ouadah, "Pipeline defects risk assessment using machine learning and analytical hierarchy process," in *2018 International Conference on Applied Smart Systems (ICASS)*. IEEE, 2018, pp. 1–6.
[13] A. Mohamed, M. S. Hamdi, and S. Tahar, "Decision tree-based approach for defect detection and classification in oil and gas pipelines," in *Proceedings of the Future Technologies Conference*. Springer, 2018, pp. 490–504.
[14] Y. LeCun, K. Kavukcuoglu, and C. Farabet, "Convolutional networks and applications in vision," in *Proceedings of 2010 IEEE International Symposium on Circuits and Systems*. IEEE, 2010, pp. 253–256.
[15] Y. Sun, W. Zuo, and M. Liu, "Rtfnet: Rgb-thermal fusion network for semantic segmentation of urban scenes," *IEEE Robotics and Automation Letters*, vol. 4, no. 3, pp. 2576–2583, 2019.
[16] C. Xing, L. Ma, and X. Yang, "Stacked denoise autoencoder based feature extraction and classification for hyperspectral images," *Journal of Sensors*, vol. 2016, 2016.
[17] D. Scherer, A. Müller, and S. Behnke, "Evaluation of pooling operations in convolutional architectures for object recognition," in *International conference on artificial neural networks*. Springer, 2010, pp. 92–101.
[18] N. Srivastava, G. Hinton, A. Krizhevsky, I. Sutskever, and R. Salakhutdinov, "Dropout: a simple way to prevent neural networks from overfitting," *The journal of machine learning research*, vol. 15, no. 1, pp. 1929–1958, 2014.
[19] X. Glorot and Y. Bengio, "Understanding the difficulty of training deep feedforward neural networks," in *Proceedings of the thirteenth international conference on artificial intelligence and statistics*, 2010, pp. 249–256.
[20] P. Baldi, "Gradient descent learning algorithm overview: A general dynamical systems perspective," *IEEE Transactions on neural networks*, vol. 6, no. 1, pp. 182–195, 1995.
[21] D. P. Kingma and J. Ba, "Adam: A method for stochastic optimization," *arXiv preprint arXiv:1412.6980*, 2014.
[22] Y. LeCun, L. Bottou, Y. Bengio, P. Haffner *et al.*, "Gradient-based learning applied to document recognition," *Proceedings of the IEEE*, vol. 86, no. 11, pp. 2278–2324, 1998.
[23] A. Krizhevsky, I. Sutskever, and G. E. Hinton, "Imagenet classification with deep convolutional neural networks," in *Advances in neural information processing systems*, 2012, pp. 1097–1105.
[24] K. Simonyan and A. Zisserman, "Very deep convolutional networks for large-scale image recognition," *arXiv preprint arXiv:1409.1556*, 2014.
[25] K. He, X. Zhang, S. Ren, and J. Sun, "Deep residual learning for image recognition," in *Proceedings of the IEEE conference on computer vision and pattern recognition*, 2016, pp. 770–778.